

Quantitative determination of major systematics in synchrotron x-ray experiments: seeing through harmonic components

C. Q. Tran,^{1*} Z. Barnea,¹ M. D. de Jonge,¹ B. B. Dhal,¹ D. Paterson,^{1,2} D. J. Cookson^{3,4} and C. T. Chantler¹

¹ School of Physics, University of Melbourne, Victoria 3010, Australia

² SRI-CAT Sectors 1–4, Argonne National Laboratory, 970 S. Cass Avenue, Argonne, Illinois 60439, USA

³ ANSTO, Private Mail Bag 1, Menai, New South Wales 2234 Australia

⁴ Chem-Mat-CARS-CAT (Sector 15, Bldg 434D), Argonne National Laboratory, 970 S. Cass Avenue, Argonne, Illinois 60439, USA

Received 5 May 2002; Accepted 9 October 2002

In line with an ongoing programme to determine accurately x-ray attenuation coefficients, we have developed a method for the quantitative determination of the effect on experimental results of monochromator harmonic components in a synchrotron beam. The technique can be adapted to suit a wide variety of experiments, and is of particular interest because it determines the effect of the harmonic components directly. This avoids the necessity for modelling and is therefore robust. Results of a direct determination of the effect of harmonic components illustrate the power of the technique. We extended the technique to quantify the effects of dark current-induced errors. Copyright © 2003 John Wiley & Sons, Ltd.

INTRODUCTION

In a pioneering report on the International Union of Crystallography (IUCr) project to resolve discrepancies between experimentally determined attenuation coefficients, Creagh and Hubbell¹ reported that in earlier experiments 'one quarter had an incident beam which may have had second-harmonic contamination' and so were rejected as a result of this. Such harmonic components occur in synchrotron and laboratory x-ray beams and are often assumed to be insignificant without explicit quantification of their amplitude or their effect on experimental results.

Monochromatic x-ray beams are required for many applications. They can be produced using radioactive sources, characteristic emission lines excited by electron bombardment or monochromatization of a polychromatic spectrum such as that of a synchrotron or laboratory source. In synchrotron environments, crystal or grating monochromators often provide the first stage of beam monochromatization. Further monochromatization is effected by detuning the second face of a double-bounce monochromator,^{2,3} by the application of further diffractive monochromatization with different harmonic orders,^{4,5} by filtering the beam through an absorber with differential attenuation at the wanted and unwanted energies⁶ or by the use of a mirror.^{7,8} In each configuration, the residual harmonic content in the beam may affect the experiment. Most configurations minimize

the harmonic component in the beam, although the reduction of the fraction by two orders of magnitude may still yield an unacceptable harmonic fraction for many studies. Mirror configurations can provide a high-energy cut-off for the synchrotron beam, eliminating any harmonic contribution, but may place unacceptable restrictions on experiments requiring a scanning of the energy. Changes in the mirror configuration also affect the beam condition from energy to energy, and the mirror loses efficacy above energies around 20 keV.⁷

Crystal monochromators select a series of harmonics whose wavelengths satisfy the Bragg equation for the diffracting planes of the monochromator. Some harmonics can be minimized by the use of diffracting planes whose second-order reflection is forbidden, as, for example, in the case of the (111) planes of silicon and germanium monochromators. Even in these cases, third-order and higher harmonics can often be present, especially when their intensity in the source spectrum is significant. Any studies in which the monochromatic nature of the x-rays is important require, therefore, a method for the quantitative determination of the harmonic component in the x-ray beam. The primary problem with many studies relating to attenuation or scattering was alluded to by Creagh and Hubbell¹ when they observed that 'if a plot of $\ln(I/I_0)$ against thickness ... does not yield a straight line then no unique x-ray attenuation coefficient exists and an investigation must take place to establish what is the cause of this non-linearity.' The spectral bandwidth affects results of any studies where the quality of the beam affects resolution, contrast, relative structure or normalization in any energy-dependent manner.

*Correspondence to: C. Q. Tran, School of Physics, University of Melbourne, Victoria 3010, Australia.
E-mail: tran@physics.unimelb.edu.au
Contract/grant sponsor: Australian Synchrotron Research Program.

A method for the absolute quantification of the beam spectrum⁹ used a solid-state detector to record the Compton scattered spectrum of aluminium and therefore hardly lends itself to quantitative determination, owing to the difficulties in accurately modelling the Compton interaction. To determine the effect of the beam spectrum on the experiment of interest, one must also make corrections to the determined spectrum for the detector response functions, geometric factors and other beamline components. Exact detector window thicknesses, gold and oxide layers must be known and, in our case, the length of the active region must be determined for all ion chambers. Chapman *et al.*'s technique⁹ is suited to the relative measurement of a continuous spectrum, calibrated using an independent detection system of energy-dispersive detectors with a different air path, followed by modelling to quantify the spectral content of a final measurement. However, the complexity of this approach does not lend the method to transparent use. Hence the effect of the harmonic components in the beam has often been left to order-of-magnitude calculations after 'minimization' by highly detuning the monochromating crystal.

A more traditional determination of the harmonic components by absorption of the monochromatized beam by multiple foils is well known in the literature.¹⁰ In this work, we developed this technique for use with synchrotron beams and ion-chamber detectors, and extended it to provide accurate knowledge of the beam spectral components. We exploit the sensitivity of the technique to quantify further the effect of dark current instabilities which may be otherwise unrecoverable within an experimental arrangement. A simple method used the rotation of a single crystal to increase the effective thickness and attenuation, and hence to investigate harmonic content, but this method has been shown to be generally liable to cause significant systematics at the 1–2% level.¹

In our method, the harmonic components are determined in-line with the desired experimental geometry and detectors and require no complex Compton calculations. We have probed the attenuation over a range corresponding to $[-30 < \ln(I/I_0) < 0]$ for the fundamental energy, far exceeding the 'recommended'¹¹ Nordfors¹¹ range of $[-4 < \ln(I/I_0) < -2]$. Sampling the linearity of the attenuation over a much wider range than in previous investigations permits a more extensive diagnosis of systematic effects including detector linearity, harmonic content, dark current offsets and saturation.

The method is able to produce quantification of the effect of harmonic component (contamination) down to the 0.01% level for the first time. Surprisingly, the harmonic contamination in numerous experiments may exceed 10% without the experimenters noticing that a major problem lies in the data. This approach is an essential ingredient in the recent investigation of copper form factor measurements.¹² This in-line technique relies on the log-linearity of the absorption of x-rays by atomic materials. Scattering cross-sections are often non-linear on such a logarithmic plot, but this non-linearity makes only a small correction in the x-ray range of energies. We begin the discussion of

the principles of the technique with a discussion of the attenuation measurement.

EFFECT OF HARMONICS IN ATTENUATION MEASUREMENT

If the detector response is perfectly linear and no harmonics are present, the logarithm of the intensity plotted as a function of the absorber thickness t falls on a straight line whose slope is the linear absorption coefficient μ of the foil material as described by the Beer–Lambert relation, where I_0 and I are the incident and attenuated intensities, respectively:

$$-\mu t = \ln \left(\frac{I}{I_0} \right) \quad (1)$$

However, $\ln(I/I_0)$ can be non-linear with thickness t due to the presence of a harmonic. For a fraction x of harmonic x-rays (with linear attenuation coefficient μ_h) in the incident monochromatized beam (with μ_f the linear attenuation coefficient for the fundamental energy), the resulting measured linear attenuation coefficient of the x-ray beam μ_{meas} will be

$$-\mu_{\text{meas}} t = \ln \left(\frac{I}{I_0} \right)_{\text{meas}} = \ln[(1-x)e^{-\mu_f t} + xe^{-\mu_h t}] \quad (2)$$

Figure 1 shows the measured attenuation of 11 sets of aluminium foils (with thicknesses between 15 μm and 1 mm) in the path of an x-ray beam monochromated by a detuned, double-bounce silicon (111) channel-cut monochromator set to select 5 keV x-rays. The uncertainty of 0.02% is the one standard deviation fitted uncertainty using Eqn (2).

The measurements were carried out by using a metal 'daisy wheel' on whose perimeter were mounted 11 different thicknesses of foils. The requirement of a precise knowledge of foil thickness was avoided by using multiples of a single foil for each of these thicknesses. In this way the ratio of thicknesses of each of the absorbers was well known. These foils were placed in the beam by suitable rotation of the daisy wheel. This technique is accurate, reproducible and

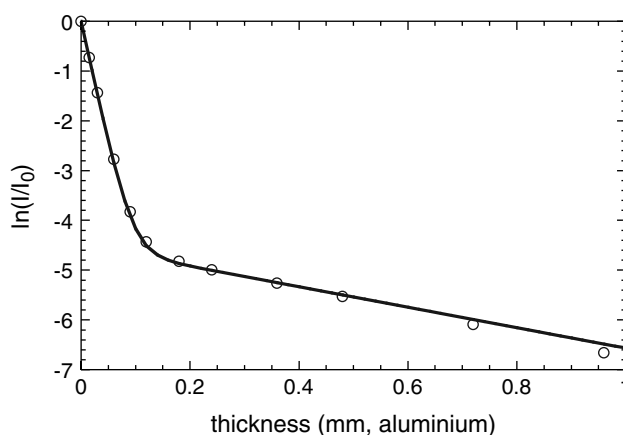


Figure 1. The attenuation, $\ln(I/I_0)$, as a function of the thickness of aluminium absorber in the x-ray beam with a silicon monochromator set to 5 keV. o, Experimental results; solid line, curve of best fit corresponding to an admixture of $(1.09 \pm 0.02)\%$ third-order harmonic (15 keV) following Eqn (2).

rapid. The monitor and detector used throughout this work were matched nitrogen gas-flow ion chambers. The work was performed at the bending magnet beamline 20B of the Photon Factory synchrotron at Tsukuba.

The experimental results follow a straight line until the thickness of aluminium increases to such an extent that the transmitted radiation consists overwhelmingly of the more energetic 15 keV third-order harmonic. When this occurs, one observes an inflection with the gradient approaching that of the linear attenuation coefficient of the sample at the energy of the third-order harmonic.

This inflection in the plot provides clear evidence for the presence of a third-order harmonic [the (222) second order reflection for silicon is 'forbidden']. The solid curve in Fig. 1 is the thickness dependence of the attenuation of aluminium for 5 keV x-rays with an admixture of $(1.09 \pm 0.02)\%$ of the 15 keV third-order harmonic, as can be confirmed by extrapolating the second 'linear' portion of the graph back to zero thickness.

Use of relatively calibrated sample thicknesses prevents us from determining the attenuations μ_f and μ_h from this measurement, but the harmonic component remains very well defined. In fact, any good attenuation measurement should be capable of probing the harmonic component of the beam if it aims to be accurate at the sub-percent level.

To perform an actual attenuation measurement in this manner, it is more efficient to use a smaller number of carefully calibrated thicknesses. A minimum of three samples of accurately known thickness is required to simultaneously determine x , μ_f and μ_h . If μ_h is provided by a separate experiment (or theory), then the use of three samples overdetermines the problem and allows for error analysis, or alternatively allows the possible observation of an additional harmonic. In Fig. 2 we have determined the harmonic components of the beam with the use of three well-calibrated foil thicknesses.¹³ Attenuation measurements of the foils at

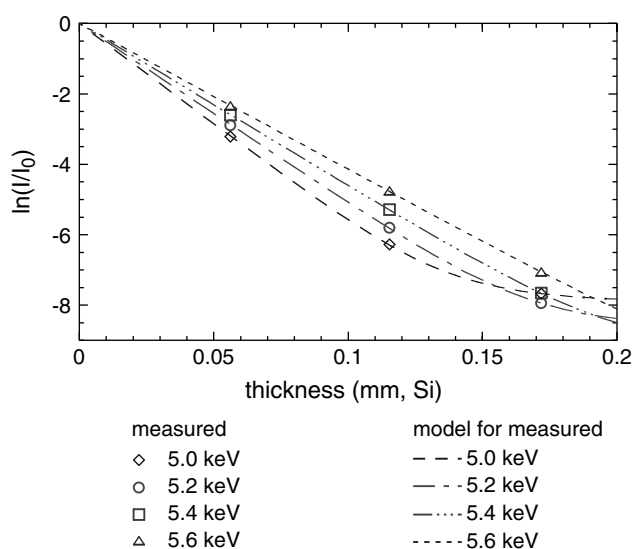


Figure 2. A harmonic component measurement with three well-calibrated thicknesses provides a constant and reliable indicator of accuracy in attenuation measurements. Error bars are given by the thickness of the line.

the harmonic energy yield a linear absorption coefficient μ_h providing the gradient for the harmonic component dominating in the high-thickness portion of the graph. This technique provides constant and reliable feedback about the condition of the beam and the accuracy of the measurement.

PRINCIPLES OF DIRECT DETERMINATION OF THE EFFECT OF HARMONIC COMPONENTS

The advantage of an 'in-line' measurement is that the same beam and counting system are used for the determination of the harmonic component and the main experiment. Hence the directly measured quantity is the effect of the harmonic components, with regard to the counters used. This situation is far preferable to an indirect measurement of the beam spectrum which must then be corrected to determine the likely effect of the harmonic components in a given detector and may have consequent errors in excess of 10%. For an indirect method to be used in this scenario, one would need to identify and exactly quantify these sensitivities.

To consider the significance of any harmonic component or any non-monochromaticity after a monochromator, we use a typical synchrotron beam-line geometry (Fig. 3) in this example and analysis. Table 1 shows the result of modelling the fraction of harmonic photons in a synchrotron beam after interactions with various beamline components. Only the first and third harmonics are shown here for brevity. The second column shows the harmonic fraction derived from an x-ray optical ray-tracing program, XOP,¹⁴ modelling the beam spectrum using operational parameters of the Australian National Beamline Facility (ANBF) beamline 20B. The third column shows the harmonic fraction after monochromation by a thick, perfect crystalline, silicon 111 double-bounce crystal monochromator. Integrated reflectivities were used, and no detuning was modelled in this calculation, as the absolute detuning angle is not well known at 20B. The modelling for this calculation was performed using the dynamic diffraction program MOSCURVE.^{15,16} As can be seen, the harmonic fraction at this stage is much reduced, and one might be tempted to suggest that it is negligible.

However, other beamline components at 20 B (Fig. 3) modify the ratio of harmonic components significantly according to standard Beer–Lambert absorption. When the effects of these components are factored into the calculation (using Ref. 17), the beam spectrum changes significantly. The penultimate column shows that the harmonic component in the beam has increased from a monochromated fraction of 1.36% to 74.5% due to the differential absorption of the fundamental and harmonic photons by the beamline elements at 5 keV. Window thicknesses and air paths are critical at lower energies, and detuning may discriminate against the harmonic component by a further two orders of magnitude. With ideal detuning an experimenter will still need to contend with harmonic fraction of around 0.75%, which can easily invalidate a range of experimental results. At higher energies harmonic fractions may be lower, dependent critically on the synchrotron and beam-line, but they would still invalidate a range of experiments if not carefully quantified.

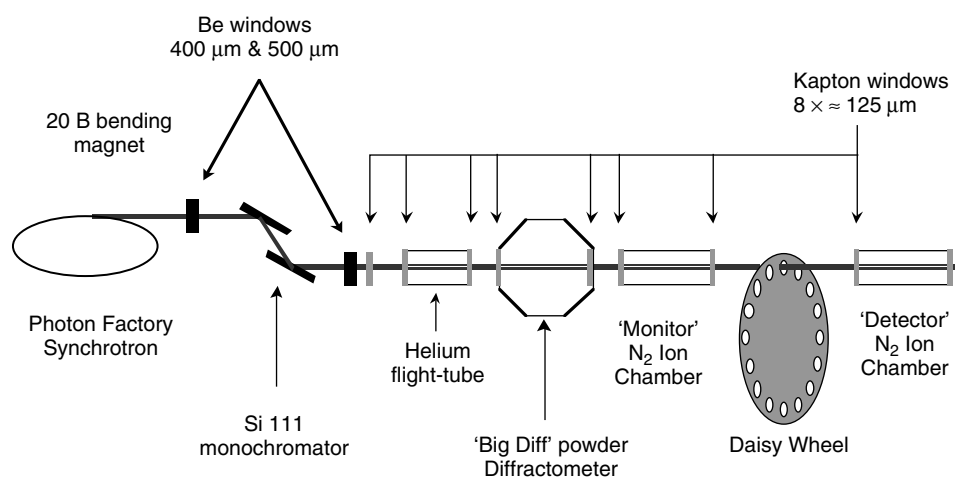


Figure 3. Beamline 20 B at the ANBF, Tsukuba. Components shown schematically for the purpose of modelling the effect of the harmonic components from the XOP modelled spectrum.

Table 1. Percentage fraction of third harmonic component at various points along a two-component synchrotron beam (modelling parameters taken from our experimental arrangement; agreement with experiment is within error)

Energy (keV)	XOP 20B simulated % of I_{3rd} in I_0	After Si 111 mono	Be windows 900 μm	Kapton windows 1000 μm	Monitor absorption 186 mm	Air path absorption 192 mm	Effective harmonic in detector I.C. 186 mm
5.0	10.8	1.36	2.48	40.6	55.8	74.5	13.7
6.0	6.89	0.833	1.17	7.27	10.1	15.4	0.961
7.0	4.33	0.509	0.630	2.02	2.51	3.39	0.200
8.0	2.69	0.311	0.358	0.783	0.907	1.11	0.0720
9.0	1.66	0.190	0.209	0.362	0.401	0.464	0.0344
10.0	1.02	0.115	0.124	0.184	0.198	0.220	0.0191

The degree to which the harmonic content is problematic will also depend on the experimental arrangement. In our experiments the detectors of choice are matched ion chambers: one is employed as a beam monitor and the other as the experimental detector. Ultimately, the presence of the harmonic components is only problematic to the degree to which we are able to detect them in this detector. Thus, the relevant figure in Table 1 is not the harmonic component in the beam immediately before the detector, but the ratio of each component absorbed by this second detector. In the case of a nitrogen-filled ion chamber, the efficiency of detection of fundamental and harmonic photons is biased, although other commonly used detectors such as CCDs have a fairly flat detector response function across a similar operating range. This consideration results in an *effective* harmonic fraction of 13.7% for a non-detuned synchrotron beam with ion-chamber detectors.

QUANTITATIVE DETERMINATION OF THE EFFECT OF HARMONIC COMPONENTS AS A FUNCTION OF DETUNING

Figure 4 shows the effect of detuning the monochromator on the beam harmonic content. The top-most curve corresponds to attenuation measurements with little (approximately zero) detuning. As the detuning is increased the harmonic component is reduced by around two orders of magnitude, as

expected. The dashed, dot-dashed and dotted curves show an effective ($18.90 \pm 0.07\%$), ($1.09 \pm 0.02\%$) and ($0.18 \pm 0.01\%$) of 15 keV, third-order harmonic in the beam, respectively, with fitted one standard deviation uncertainties. The upper curve corresponds approximately to the situation modelled in Table 1 at an energy of 5 keV. These results agree within uncertainties of the window and air path components in the beam path. Note that the experimental results are sufficiently sensitive to observe 0.18% levels of contamination, and they are able to quantify such non-linearity to an uncertainty of 0.01%. The advantages of the current method are that it can observe any non-linearity to below 0.05% and quantify the effect of this to below 0.01%.

DARK CURRENT

The highly detuned data in Fig. 4 show a downturn away from a straight line for high attenuation thicknesses, away from the expected gradient μ_h . This is the result of an inadequately determined dark current offset.

Dark current is the background signal measured in a detector in the absence of an x-ray beam. Often measurements are made in such a way that the 'true' counts are a result of a subtraction of the experimental counts and the dark current, which is measured before or after the experimental signal. The level of the dark current depends on experimental settings (such as gain and offset current in the

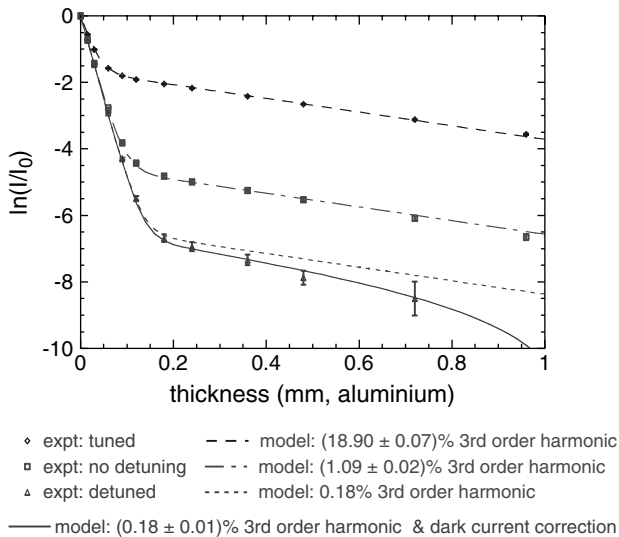


Figure 4. The effect of tuning and detuning the monochromator compared with the default detuning (all measurements at 5 keV).

context of ion chambers) or on experimental parameters, such as the temperature of a CCD camera.

In line with our technique, the effect of an incorrect dark current determination is examined in the context of an attenuation measurement. It appears in such a measurement according to

$$-\mu_{\text{meas}}t = \ln\left(\frac{I}{I_0}\right)_{\text{meas}} = \ln\left(\frac{I - I_{\text{dc}}}{I_0 - I_{0,\text{dc}}}\right) \quad (3)$$

where $I_{0,\text{dc}}$ and I_{dc} are the estimated dark currents associated with the incident and attenuated beams, respectively. The effect of saturation is given in Ref. 18 and can be demonstrated to have a signature orthogonal to those for the dark current and harmonic systematics.

If the dark current is under- or over-estimated then the measured attenuation curves will be distorted for highly attenuating samples. In the highly detuned case from the preceding section, we can see the effect of an incorrectly interpolated dark current as the transmitted intensity approaches the measured dark current level. In this case we modelled a further dark current offset (a correction to the dark current level) to explain the divergence of these curves. The dark current 'drift' is thus explained by a correction from, e.g., 840 counts to, e.g., 804 counts for the dark current level.

The competing effects of harmonic content and dark current fluctuations in the beam and detection system can be clearly distinguished in the high attenuation regime by such a study. This is achieved by recognizing that the harmonic components give rise to two linear regions separated by a transition region in the attenuation versus thickness plot. Dark current effects, on the other hand, are a function of $\ln(I - I_{\text{dc}})$ and are thus non-linear with thickness.

Similarly, one may note that the remaining dominant source of error in (detection plus beam) systems is detector non-linearity. This effect is not localized in the high attenuation region of the attenuation versus thickness plot

as are harmonic components and dark current effects. The remaining detector non-linearities may be an ugly function of count rate or may be confined to the high-counting region, where saturation effects may dominate. A non-linear middle region generally invalidates a measurement unless the detector can be calibrated. The linearity of the attenuation versus thickness plot would provide an excellent means by which to prove an optimized detection system for any experiment.

DISCUSSION

We have shown that the multiple foil method can be used as a sensitive diagnostic method for the determination of the effective fraction of harmonic radiation in a monochromatized x-ray beam. The method can simultaneously provide quantitative information about non-linear detector response such as may occur at high and low counting rates.

The incident intensity I_0 and the attenuation ratio I/I_0 must lie within a reasonable range to maintain statistical precision. The Nordfors¹¹ criterion suggests that the attenuation ratio should be in a relatively narrow range $[-4 < \ln(I/I_0) < -2]$ to optimize counting statistics, and has been widely used in the field. However, Fig. 5 shows that this criterion will lead to a significant and undiagnosable error in the presence of even fairly small (e.g. 0.18%) effective percentages of higher order harmonics. Sampling a wide range of attenuations is essential to diagnose these problems down to the 0.01% level, so the earlier criterion is generally inadequate. This approach is an essential ingredient in the recent investigation of copper form factor measurements.^{12,19}

The simplicity of the method and the ease with which it can be automated renders it suitable as a test in a large variety of experiments. Although our examples presented situations in which a single additional harmonic was

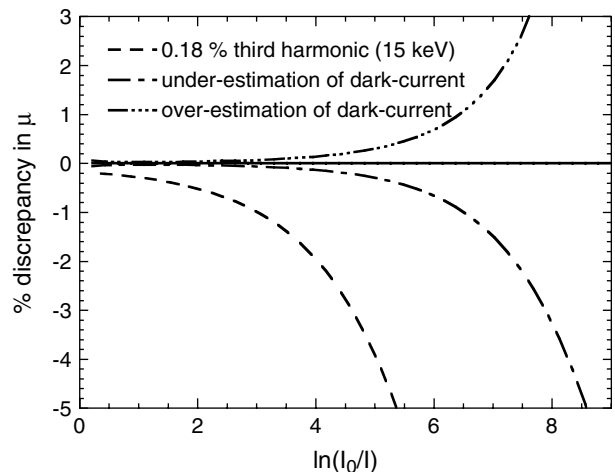


Figure 5. Calculated percentage deviation in the attenuation coefficient of silicon at 5 keV (zero line) due to: 0.18% admixture of third-order 15 keV harmonic (dotted line); under-estimation of dark current (dash-dotted line); and over-estimation of dark current (dash-dot-dot-dotted line). Saturation effects will affect the low attenuation region of this plot and will thus be clearly separated from those of harmonic components and dark current fluctuations.

detected, the method can be extended to analyse beams with multiple components.

Acknowledgments

We acknowledge encouragement in this work from D. C. Creagh, R. F. Garrett and J. R. Hester. This work was performed at the Australian National Beamline Facility with support from the Australian Synchrotron Research Program, which is funded by the Commonwealth of Australia under the Major National Research Facilities programme.

REFERENCES

1. Creagh DC, Hubbell JH. *Acta Crystallogr.* 1987; **7**: 102.
2. Materlik G, Kostroun VO. *Rev. Sci. Instrum.* 1980; **51**: 86.
3. Stümpel J, Becker P. *Nuovo Cimento D* 1997; **2–4**: 489.
4. Beaumont JH, Hart M. *J Phys. E* 1974; **7**: 823.
5. Bonse U, Materlik G, Schröder W. *J. Appl. Crystallogr.* 1976; **9**: 223.
6. Kanter EP, Dunford RW, Krässig B, Southworth SH. *Phys. Rev. Lett.* 1999; **83**: 508.
7. Caciuffo R, Melone S, Rustichelli F, Boeuf A. *Physics Reports* 1987; **152**: 1–71.
8. Alkire RW, Sagurton M, Michaud FD, Trela WJ, Bartlett RJ, Rothe R. *Nucl. Instrum. Methods Phys. Res. A* 1995; **352**: 535.
9. Chapman D, Moulin H, Garrett RF. *Rev. Sci. Instrum.* 1992; **63**: 893.
10. Barnea Z, Mohyla J. *J. Appl. Crystallogr.* 1974; **7**: 298.
11. Nordfors B. *Ark. Fys.* 1960; **18**: 37.
12. Chantler CT, Tran CQ, Paterson D, Cookson DJ, Barnea Z. *Phys. Lett. A* 2001; **286**: 338.
13. Tran CQ, Chantler CT, Barnea Z, Patterson D, Cookson DJ. To be published.
14. Dejus RJ, Sanchez del Rio M. *Rev. Sci. Instrum.* 1996; **67**: 3356.
15. Chantler CT. *J. Appl. Crystallogr.* 1992; **25**: 674.
16. Chantler CT, Deslattes RD. *Rev. Sci. Instrum.* 1995; **66**: 5123.
17. Chantler CT. *J. Phys. Chem. Ref. Data* 1995; **24**: 71.
18. Chantler CT, Staudenmann JL. *Rev. Sci. Instrum.* 1995; **66**: 1651.
19. Chantler CT, Barnea Z, Tran CQ, Tiller J, Paterson D. *Opt. Quantum Electron* 1999; **31**: 495.